Audio Engineering Society

Convention Paper

Presented at the 123rd Convention
2007 October 5–8 New York, NY

Rendering of virtual sound sources with arbitrary directivity in higher order Ambisonics

Jens Ahrens, Sascha Spors

Deutsche Telekom Laboratories, Technische Universität Berlin, Ernst-Reuter-Platz 7, 10587 Berlin, Germany

Correspondence should be addressed to Jens Ahrens (jens.ahrens@telekom.de)

ABSTRACT

Higher order Ambisonics (HOA) is a spatial audio reproduction technique aiming at physically synthesizing a desired sound field. It is based on the expansion of sound fields into orthogonal basis functions (spatial harmonics). In this paper we present an approach to the two-dimensional reproduction of virtual sound sources at arbitrary positions having arbitrary radiation directivities. The approach is based on the description of the directional properties of a source by a set of circular harmonics. Consequences of truncation of the circular harmonics expansion and spatial sampling as occurring in typical installations of HOA systems due to the employment of a finite number of loudspeakers are discussed. We illustrate our findings with simulated reproduction results.

1. INTRODUCTION

Higher order Ambisonics (HOA) is a sound reproduction technique that utilizes a large number of loudspeakers to physically recreate a sound field in a specific listening area. This desired sound field is typically described via its spatial harmonics expansion coefficients [5]. These can be yielded either from appropriate microphone recording techniques which utilize a Fourier series representation of the recorded signals [7] or virtual sound scenes may be composed of a number of virtual sound sources whose spatial harmonics expansion coefficients are derived from analytical source models. In this paper we will concentrate on the latter case. In the context of wave field synthesis, another physically based audio reproduction technique, the rendering of analytically described virtual scenes is termed *model based rendering* complementary to *data based rendering* when the rendered scene has been recorded [10].

So far virtual sources have typically been modeled as emitting plane or spherical waves whereby some further extensions exist (confer to section 2). This circumstance does not exploit all potentials of HOA since directional properties of sound sources are

known to contribute to immersion and presence of a sound scene.
Although the basic principle of HOA directly suggests the coding of the directional properties of virtual sound sources via spatial harmonics, as we propose it, we are not aware of an according explicit description in the literature. For wave field synthesis a similar approach has recently been presented by the authors [1].
Our approach focusses on two-dimensional reproduction. However, an extension to three dimensions is straightforward.

1.1. Nomenclature

In the remainder of this paper we will assume that the near field correction is included in the Ambisonics approach as described in section 2. Thus, when we speak of Ambisonics we implicitly mean near field corrected higher order Ambisonics (NFC-HOA) except where otherwise stated.
The following conventions are used: For scalar variables lower case denotes the time domain, upper case the temporal frequency domain. Vectors are denoted by lower case boldface. The descriptions in this paper are restricted to two-dimensional reproduction which means in this context that an observed sound field is independent from one of the spatial coordinates, e.g. $P(x, y, z, \omega) = P(x, y, \omega)$. The two-dimensional position vector in Cartesian coordinates is given as $\mathbf{x} = [x \; y]^T$. The Cartesian coordinates are linked to the polar coordinates via $x = r \cos\alpha$ and $y = r \sin\alpha$. The acoustic wavenumber is denoted by k. It is related to the temporal frequency by $k = \left|\frac{\omega}{c}\right|$ with ω being the radial frequency and c the speed of sound.
Outgoing monochromatic plane and cylindrical waves are denoted by $e^{-j\frac{\omega}{c}(x\cos\theta_{\text{pw}}+y\sin\theta_{\text{pw}})}$ and $H_0^{(2)}(\frac{\omega}{c}r)$ respectively, with θ_{pw} being the propagation direction of the plane wave.

2. THE AMBISONICS APPROACH

In the typical HOA approach both the desired sound field as well as the sound fields emitted by the loudspeakers are expanded into Fourier series with respect to the positional angle [4]. This results in an equation system that is solved for the optimal loudspeaker driving signals that drive the loudspeakers such that their superposed sound fields best approximate the desired one in a given sense, e.g. least square error (LSE). The term Ambisonics traditionally refers to first order Ambisonics, thus involving a tetrahedron of loudspeakers. "First order" because this setup is restricted to the reproduction of zeroth and first order spatial harmonics only [4]. Setups involving more loudspeakers and thus providing the ability to reproduce also harmonics of a higher order than one are termed HOA.
In the early years the Ambisonics community has focussed on plane waves as analytic sound field model both for the virtual sources and the loudspeakers. This framework heavily restricts the versatility of HOA. Although the reproduction over an extended listening area is targeted the reproduction quality deteriorates heavily as the listener departs from the central listening spot. Even there the curvature of the synthesized wave front deviates strongly from the desired one [2].
Recent extensions have included a compensation for the properties of the sound field of a finite distance source for both virtual sources and loudspeakers. This highly ameliorated the reproduction quality especially for off-center listening [2]. These extensions are typically termed near field corrections and the resulting system consequently near field corrected HOA (NFC-HOA). The near field correction enables the ability to synthesize a desired wave front over an extended listening area. Contrary to wave field synthesis this listening area becomes smaller with higher frequency given a certain tolerated deviation. NFC-HOA furthermore enables the rendering of virtual spherical waves [2]. Thus, it makes it possible to also assign a distance to a virtual sound source and not only a direction. The rendering of simple directive sources is addressed in [8].
The Ambisonics approach is usually divided into an encoding and a decoding stage. In the former the spatial information about the sound field to be reproduced, i.e. its spatial spectrum, is reduced by limiting the spatial bandwidth. In this framework (the so-called 'Ambisonics' domain) the signals can then be more or less efficiently stored or transmitted independently from the loudspeaker layout.
In the decoding stage the 'Ambisonics' signals are then adopted to the actual loudspeaker layout to be rendered. Apart from the inconvenience of an additional intermediate processing stage, the decomposition of the Ambisonics approach into en- and decoding brings another disadvantage. It is the fact

that the filters necessary for the near field correction are unstable if only the encoding stage is considered. Although workarounds are given in [2] we consider this decomposition as cumbersome in the context of this paper. For ease of illustration we will thus skip the encoding/decoding procedure and directly derive the loudspeaker driving signals from the initial virtual sound field description. We will follow the procedure outlined in [10]. Similar to the terminology used in wave field synthesis we will rather speak of a driving function than of an Ambisonics signal.
To illustrate Ambisonics it is typically assumed that the secondary sources are located on a sphere around the listener residing in the center, since a closed solution for the loudspeaker driving functions can be derived for this setup. Note that also irregular setups can be handled [7].
In the two-dimensional reproduction scenario considered here, the secondary sources are located on a circle. For convenience, we assume an evenly spaced distribution of N loudspeakers around the origin of the coordinate system as depicted in Fig. 1. The reproduced wave field is given as

$$P(\mathbf{x},\omega) = \sum_{n=0}^{N-1} D(\alpha_n, R, \omega) \cdot V(\mathbf{x}, \mathbf{x}_n, \omega) \; , \qquad (1)$$

where $D(\alpha_n, R, \omega)$ denotes the driving signal for the n-th secondary source situated at $\mathbf{x}_n = R \cdot [\cos\alpha_n \quad \sin\alpha_n]^T$ and $V(\mathbf{x}, \mathbf{x}_n, \omega)$ its spectrum. $\alpha_n = n\frac{2\pi}{N}$. Note that the temporal source spectrum is inherently included in the driving functions $D(\alpha_n, R, \omega)$. These are derived by setting the left hand side of (1) to the desired wave field and solving the resulting equation with respect to $D(\alpha_n, R, \omega)$ as it is performed in section 3.1.

3. DERIVATION OF THE DRIVING FUNCTION

3.1. Mode-Matching Approach

In the context of this paper we define the directivity of a sound source as its temporal impulse response, i.e. the sound field created by the source when is it fed by a temporal impulse.
Any arbitrary two-dimensional virtual source sound field $S(\mathbf{x},\omega)$ can be decomposed into circular harmonics, so can the above defined directiviy. This decomposition is the two-dimensional analogon of

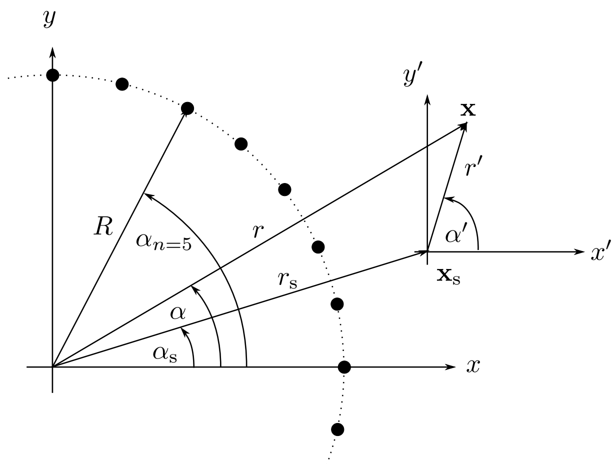

Fig. 1: The coordinate systems used in this paper. The dots • denote the positions of the secondary sources.

the cylindrical harmonics expansion [15]. Its favorable properties in our context are: (a) It provides an orthogonal expansion of the virtual source field, (b) rotations of the virtual source can be simply expressed by phase shifts, and (c) the expansion coefficients can be easily derived from the far-field (plane wave) characteristics of the virtual source via a Fourier transformation [11].
For a virtual source located at $\mathbf{x}_s$ this decomposition yields

$$S(\mathbf{x},\omega) = \hat{S}(\omega) \times \times \sum_{\eta=-\infty}^{\infty} \breve{S}^{(2)}(\eta,\omega) H_\eta^{(2)}(\frac{\omega}{c} r') e^{j\eta\alpha'} \; , \qquad (2)$$

where $\hat{S}(\omega)$ denotes the temporal source spectrum (i.e. the input signal) and $H_\eta^{(2)}$ the η-th order Hankel function of second kind. The coefficients $\breve{S}^{(2)}$ are termed circular harmonics expansion coefficients. The coordinates $r' = r'(\mathbf{x})$ and $\alpha' = \alpha'(\mathbf{x})$ belong to a local coordinate system whose origin coincides with the source's location $\mathbf{x}_s$ and whose axes are parallel to the global x- and y-axes (cf. to figure 1). The infinite sum on the right hand side of (2) fully describes the source's directivity. Note that $\hat{S}(\omega)$ and $\breve{S}^{(2)}$ may also be combined. But for ease of illustration we keep them separated.
However, in order to apply the Ambisonics approach

introduced by (1) we seek for an expansion of the source's directivity at the origin of the global coordinate system, thus an expansion in r and α. We therefore apply the addition theorem for cylinder harmonics [13] to translate the expansion from (2) to our global origin:

$$S(\mathbf{x},\omega) = \hat{S}(\omega) \cdot \sum_{\eta=-\infty}^{\infty} \breve{S}^{(2)}(\eta,\omega) \times$$
$$\times \sum_{\nu=-\infty}^{\infty} J_\nu(\frac{\omega}{c}r) H^{(2)}_{\nu-\eta}(\frac{\omega}{c}r_\mathrm{s}) e^{-j(\nu-\eta)\alpha_\mathrm{s}} e^{j\nu\alpha} \ . \quad (3)$$

Note that our nomenclature and definition of incoming and outgoing waves (confer to section 1.1) alters the theorem given in [13] to the form being evident in (3). Note also that (3) is only valid for $r < r_\mathrm{s}$.
Incorporating (3) as desired sound field into (1) and modeling the loudspeakers as line sources, i.e.

$$V(\mathbf{x},\mathbf{x}_n,\omega) = \frac{j}{4} H_0^{(2)}(\frac{\omega}{c}|\mathbf{x}-\mathbf{x}_n|) \ , \quad (4)$$

and expanding $H_0^{(2)}(\frac{\omega}{c}|\mathbf{x}-\mathbf{x}_n|)$ about the global origin via the addition theorem applied in (3) leads to the relationship

$$-4j\cdot\hat{S}(\omega)\cdot \sum_{\eta=-\infty}^{\infty} \breve{S}^{(2)}(\eta,\omega) \frac{H^{(2)}_{\nu-\eta}(\frac{\omega}{c}r_\mathrm{s})}{H^{(2)}_{\nu}(\frac{\omega}{c}R)} e^{-j(\nu-\eta)\alpha_\mathrm{s}} =$$
$$= \underbrace{\sum_{n=0}^{N-1} D(\alpha_n,R,\omega) e^{-j\nu n \frac{2\pi}{N}}}_{=\mathrm{DFT}_N\{D(\alpha_n,R,\omega)\}} \qquad \forall\ \nu \ . \quad (5)$$

Note that (5) essentially demonstrates the so-called mode matching approach commonly applied in similar problems [7]. The right hand side of (5) can be interpreted as a discrete Fourier series (DFS) expansion of period N with respect to n. It may also be interpreted as a discrete Fourier transform (DFT) of length N with respect to n. The difference between both alternatives is the definition for values of n outside the interval $[0;\ N-1]$. The DFS expansion assumes the signal to be periodic whereas the DFT assumes it to be zero for $n \ni [0;\ N-1]$ [9]. In our case n will never exceed $[0;\ N-1]$ so we do not need to bother and may choose the DFT for convenience since we assume more familiarity of the reader with DFT rather than with DFS.

Thus, to yield $D(\alpha_n,R,\omega)$ we need to perform an inverse DFT (IDFT) with respect to ν on both sides of (5) reading

$$D(\alpha_n,R,\omega) = -4j\cdot\mathrm{IDFT}_N\left\{\sum_{\eta=-\infty}^{\infty}\breve{S}^{(2)}(\eta,\omega)\ \times\right.$$
$$\left.\times\ j^{-\nu}\frac{H^{(2)}_{\nu-\eta}(\frac{\omega}{c}r_\mathrm{s})}{H^{(2)}_{\nu}(\frac{\omega}{c}R)} e^{-j(\nu-\eta)\alpha_\mathrm{s}}\right\}\cdot\hat{S}(\omega) \ . \quad (6)$$

The factor $j^{-\nu}$ was introduced due to the fact that the inverse DFT in (6) has to be performed symmetrically from $\nu = -\frac{N-1}{2}$ to $\nu = \frac{N-1}{2}$ for odd N and accordingly for even N, and not from 0 to $N-1$ like the forward DFT in (5) [9]. Due to the repeated application of the addition theorem for cylinder harmonics (confer to (3)) equation (6) is only valid for $r < r_<$, whereby $r_<$ is the smaller of r_s and R.
Note that although all equations above employ the equality sign, this does not imply that the reproduced sound field is equal to the desired (virtual) one. Confer to section 4 for a further discussion.
To approximate Hankel functions via expressions which can be efficiently implemented via simple filtering and delaying of a signal, the large argument approximation for the Hankel function is commonly applied. One is now tempted to pose the restriction on the position $\mathbf{x}_\mathrm{s}$ of the virtual source to be far enough from the origin so that this large argument approximation for the Hankel function holds. But due to the fact that in (6) the dependent variable is the order of the Hankel functions and not the argument it is not admissible. Doing so will result in a plane wave carrying along a single component of the directivity of the virtual source, the one pointing towards the reference point (i.e. the origin of the coordinate system in our case).

3.2. Sound field manipulations

Apart from generally changing the source's directivity three different elementary manipulations of the virtual sound field are possible: (a) rotation of the source around the origin of the coordinate system, (b) translations of the sound source radially with respect to the origin of the coordinate system, and (c) rotation of the sound source about its location.
Manipulations in terms of (a) simply add a linear phase value to the argument of the IDFT in (6), thus continuously rotate the loudspeakers signals around

the array. For manipulations in terms of (b) the argument of the IDFT in (6) has to be evaluated. Rotations of the virtual source about its location (case (c)) can be achieved by introducing the complex factor $e^{-j\eta\alpha_{\mathrm{rot}}}$ into the expansion in (2), thus adding a constant phase value to the argument of the IDFT in (6). α_{rot} denotes the angle by which the source is rotated.

4. TRUNCATION OF THE HARMONIC EXPANSION AND SPATIAL SAMPLING

The transition from equation (5) to (6) truncates the reproducible spatial bandwidth to modes from $\nu = -\frac{N-1}{2}$ to $\nu = \frac{N-1}{2}$ for odd N and accordingly for even N. Generally, a virtual sound field will have energy outside this interval. This truncation obviously produces spatial artefacts. However, extending the range of reproduced spatial modes potentially reduces these artefacts.

To quantify the truncation error the *normalized truncation error* was introduced in [14] as the ratio of the reproduction error and the desired sound field. The reproduction error is the difference of the desired sound field and the actual reproduced sound field. Both numerator and denominator are integrated over the unit circle. In [14] results are given for a sample plane wave, in [7] for a sample spherical wave. Both examples show similar qualitative and even quantitative reduction of the error with extension of the modal bandwidth. Similar tendencies can be assumed for arbitrary virtual sources.

As outlined in [6] there are strong indications that there exists a threshold above which only little improvement is achieved for a given listening area and frequency when the range N of rendered spatial modes is further extended.

Additionally to the truncation error artefacts due to the sampled nature of the reproduced sound field have to be expected. To investigate the sampling of the reproduced sound field due to the employment of a finite number of secondary source we will revisit the basic Ambisonics approach and reformulate it for a continuous secondary source distribution on which sampling is performed.

With this continuity assumption of the secondary source distribuion equation (1) reads

$$P(\mathbf{x},\omega) = \int_0^{2\pi} D(\alpha,R,\omega)\cdot V(\mathbf{x},\mathbf{x}_\alpha,\omega)d\alpha \ . \tag{7}$$

Performing the steps outlined in section 3.1 we arrive at the continuous equivalent of (5) reading

$$-4j\cdot\hat{S}(\omega)\cdot\sum_{\eta=-\infty}^{\infty}\breve{S}^{(2)}(\eta,\omega)\frac{H^{(2)}_{\nu-\eta}(\frac{\omega}{c}r_{\mathrm{s}})}{H^{(2)}_{\nu}(\frac{\omega}{c}R)}e^{-j(\nu-\eta)\alpha_{\mathrm{s}}} = \\ = \underbrace{\int_0^{2\pi} D(\alpha,R,\omega)e^{-j\nu\alpha}d\alpha}_{=2\pi\cdot\mathring{D}(\nu,R,\omega)} \qquad \forall\ \nu\ . \tag{8}$$

The right hand side of equation can be interpreted as a continuous inverse Fourier series (IFS) expansion of $D(\alpha,R,\omega)$ yielding the Fourier series coefficients $\mathring{D}(\nu,R,\omega)$ [11]. We model the sampling of the continuous driving function $D(\alpha,R,\omega)$ by a multiplication with a polar pulse train as

$$D_{\mathrm{s}}(\alpha,R,\omega) = D(\alpha,R,\omega)\cdot ⊥⊥⊥(\alpha) = \\ = D(\alpha,R,\omega)\cdot\sum_{n=0}^{N-1}\delta(\alpha-\frac{n}{N}2\pi)\ . \tag{9}$$

The subscript s indicates sampling. It turns out that this multiplication results in

$$\mathring{D}_{\mathrm{s}}(\nu,R,\omega) = \sum_{n=-\infty}^{\infty}\mathring{D}(\nu+nN,R,\omega)\ . \tag{10}$$

Thus, the angular sampling results in repetitions of the angular spectrum $\mathring{D}(\nu,R,\omega)$. As discussed in [11] these repetitions overlap and give rise to spatial aliasing artefacts. In our case $\mathring{D}(\nu,R,\omega)$ is given by the left hand side of (8). It can be seen that $\mathring{D}(\nu,R,\omega)$ differs from zero at any frequency ω, at any distance r from the origin, and for any order ν. Thus, spatial aliasing can not be avoided since the overlaps will always interfere. It is indeed such that extending the range of reproduced orders ν (i.e. increasing the number of loudspeakers) shifts the significant values of the involved (higher order) Hankel functions and thus the significant aliasing artefacts to higher frequencies respectively to farther distances from the coordinate origin. In the present case of directional sources the orders of the involved Hankel functions are not only dependent on the angular mode ν but also on the expansion of the source's directivity, i.e. on η (confer to equation (8)). Thus, it can be stated that the wider the range of modes of which the source's directivity is composed of, the more lower order Hankel functions are present at high angular modes ν. And consequently, the wider the range of directivity modes the lower the frequency respectively the closer the distance to the coordinate origin is where significant overlaps and thus spatial aliasing occur.

Note that the approach described in this paper provides potential to reduce spatial aliasing artefacts since it allows for an arbitrary limitation of the spatial bandwidth of the virtual sound field by limiting the range of angular modes η of the expansion of the source's directivity (equation (2)). See also [12] for a closer look.

5. DERIVATION OF A DESIRED DIRECTIVITY'S EXPANSION COEFFICIENTS

In this section will briefly illustrate how the circular expansion coefficients $\breve{S}^{(2)}(\eta,\omega)$ of a desired source directivity can be derived from a given far-field directivity pattern. Similar to the circular harmonics expansion presented in (2) any arbitrary sound field may also be expanded into its plane wave components. Applied on source fields this plane wave decomposition (PWD) describes the far-field radiation characteristics of the respective source.

A very intuitive manner of illustrating directivities are polar plots. These are frequently used to illustrate the directivities of e.g. microphones and loudspeakers and therefore many people are familiar with them. Analytically spoken polar plots represent the PWD of a directivity at a selected frequency by showing the magnitude of the PWD over all angles in a plane. To yield the circular expansion coefficients for a given PWD the following expression can be used [11]:

$$\breve{S}^{(2)}(\eta,\omega) = \frac{k}{8\pi^2} \int_0^{2\pi} j^{-\eta} \bar{S}(\theta,\omega) e^{-j\eta\theta} d\theta \ , \qquad (11)$$

whereby $\bar{S}(\theta,\omega)$ denotes the PWD of the source's directivity.

We will now illustrate the application of (11) via a simple example. One of the elementary types of directive sources is a dipole exhibiting a figure-of-eight directivity. Its normalized polar plot is given in figure 2.

When assuming far field conditions the frequency

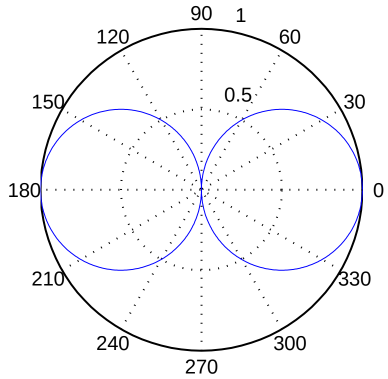

Fig. 2: Normalized polar plot of the directivity of a dipole.

response of a two-dimensional dipole is proportional to $1/\sqrt{k}$, whereby we assume k being dimensionless for convenience. The PWD of the directivity reads then

$$\bar{S}^{(2)}_{\text{dipole}}(\theta,\omega) = \frac{1}{\sqrt{k}} \cos\theta \ . \qquad (12)$$

Inserting (12) into (11) and applying Euler's identity yields that $\breve{S}^{(2)}_{\text{dipole}}(\eta,\omega)$ only differs from zero for $\eta = 1$ and $\eta = -1$, more exactly

$$\breve{S}^{(2)}_{\text{dipole}}(\eta,\omega) = \begin{cases} -\frac{j\sqrt{k}}{8\pi} & \text{for } \eta = 1 \\ \frac{j\sqrt{k}}{8\pi} & \text{for } \eta = -1 \\ 0 & \text{elsewhere} \ . \end{cases} \qquad (13)$$

6. RESULTS

In this section we simulate the implementation of a dipole as described by equations (12) and (13) to illustrate the above derived observations.

Note that the infinite sum in (6) reduces to two components in this case. The sound field of such a dipole and the sound field of an Ambisonics system rendering it are shown in figure 3(a) respectively 3(b). Here, a circular array of 56 monopole sources and a radius of 1.5 m is modeled. The geometrical parameters are chosen in accordance to the loudspeaker

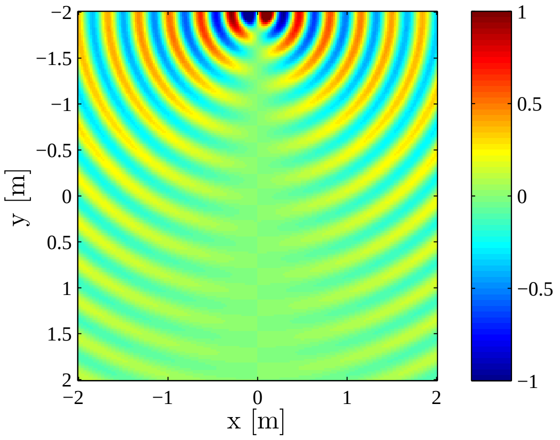

(a) Wave field $\Re\{P_{\text{dipole}}(\mathbf{x},\omega)\}$ of a dipole situated at $\mathbf{x}_\text{s} = [0\ \ -2]^T$.

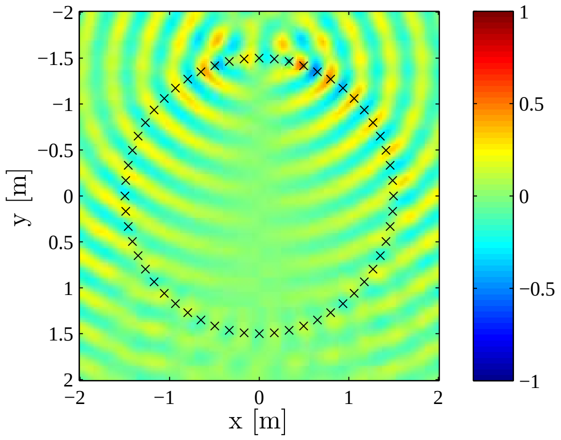

(b) Wave field $\Re\{P_{\text{Amb}}(\mathbf{x},\omega)\}$ of an Ambisonics system rendering the dipole from figure 3(a). The marks indicate the positions of the secondary sources.

Fig. 3: Simulation results for a source outside the loudspeaker array. The sound fields are scaled to have comparable levels. The values are clipped as indicated by the color bar.

system installed at the Usability Laboratory of the Deutsche Telekom Laboratories.

The emitted signal is monochromatic with a frequency of 1000 Hz. The marks in figure 3(b) indicate the secondary sources. Outside the array where (6) does not hold the two wave fields do not coincide since the propagation direction of the sound fields emitted by some of the loudspeakers does not coincide with that of the virtual source field. Inside the array a good concordance can be seen. Figure 4 further illustrates this. It shows the ratio of the two sound fields in logarithmic scale.

Note that figure 4 illustrates a fundamental difference of the capability of Ambisonics to render directional sources compared to wave field synthesis. As outlined in [1] practical implementations of wave field synthesis systems limit the reproducible spatial fine structure of sound field such that e.g. zeros in the directivity (as with dipoles) can not be rendered properly. In the present case of Ambisonics spatial aliasing and artefacts of truncation are also present but so subtile that they can only be identified in the vicinity of the loudspeakers in figure 4.

Note that it is also possible to render sources inside the listening area as illustrated in figure 5. In that case r_s is the limiting factor in equation (6) which is then only valid for $r < r_\text{s}$. Note that the loudspeakers can exhibit extremely high levels. This circumstance heavily restricts the applicability since the proper interference of the loudspeaker sound fields inside the valid listening area is very sensitive towards variation of the loudspeaker characteristics, their exact arrangement, and the acoustical properties of the reproduction room. This is typical for Ambisonics synthesis of sources inside the loudspeaker array [3].

7. CONCLUSIONS

The two-dimensional rendering of virtual sound sources with arbitrary directivity in NFC-HOA has been shown. The presented approach relies on the expansion of the directive properties of the virtual sound source into circular harmonics. A closed form solution the loudspeaker driving signals for evenly spaced circular arrays is provided. Further analysis revealed that a wider range of circular expansion coefficients of the source's directivity brings significant spatial aliasing artefacts down to lower frequencies respectively closer to the origin of the coordinate system (the reference listening position). This is due to the fact that the unavoidable overlaps in the angular spectrum of the loudspeaker driving signals cause interferences of lower order Hankel functions

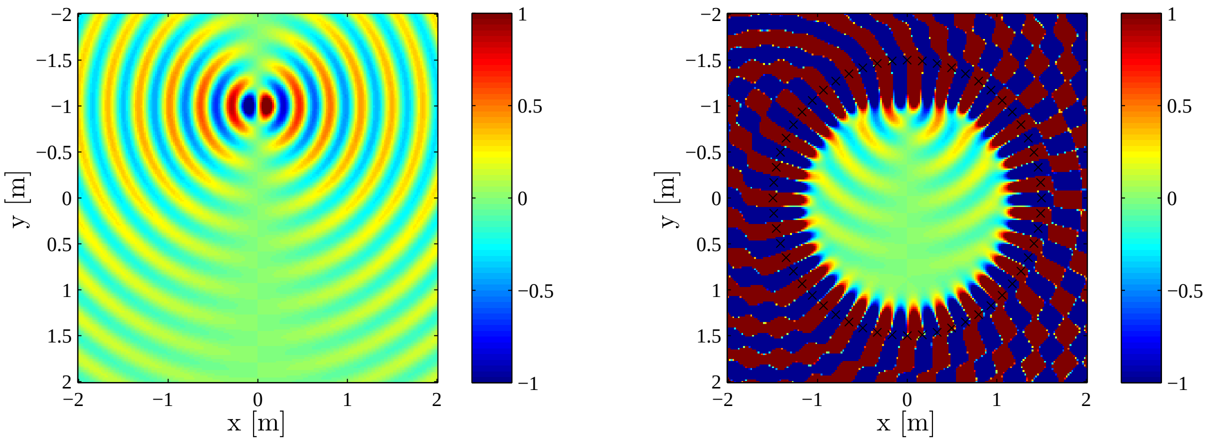

(a) Wave field $\Re\{P_{\text{dipole}}(\mathbf{x},\omega)\}$ of a dipole situated at $\mathbf{x}_s = [0 \ -1]^T$.

(b) Wave field $\Re\{P_{\text{Amb}}(\mathbf{x},\omega)\}$ of an Ambisonics system rendering the dipole from figure 5(a). The marks indicate the positions of the secondary sources.

Fig. 5: Simulation results for a source inside the loudspeaker array. The sound fields are scaled to have comparable levels. The values are clipped as indicated by the color bar.

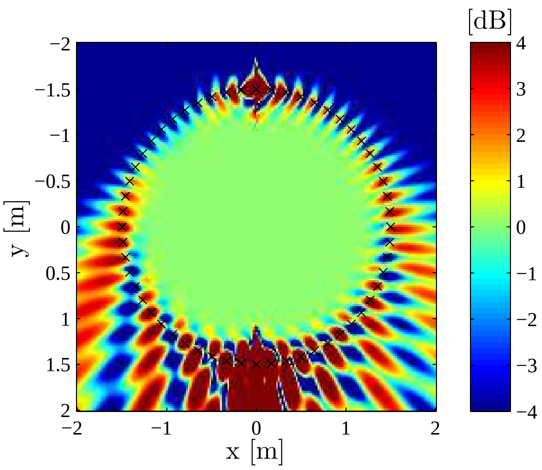

Fig. 4: Ratio of the two sound fields from figure 3 in logarithmic scale. The marks indicate the positions of the secondary sources. The values are clipped as indicated by the color bar.

which have significant values at low frequencies respectively close distances.
The two-dimensional descriptions in this paper are primarily meant as a means to illustrate the underlying physical and mathematical principles. Two-dimensional reproduction as outlined here is not suitable for implementation since appropriate loudspeakers (i.e. line sources) are hardly available. Although equation (6) provides potential for optimization of the computational complexity especially when large numbers of loudspeakers and circular expansion coefficients are involved we will not focus on this due to the above mentioned reasons.
We will rather concentrate on extending the theory to three dimensions and apply optimizations for special cases there (e.g. reproduction in a plane). Furthermore, we will give more explicit insight into the consequences of the sampled nature of the reproduced sound field which have been briefly discussed in section 4.

8. REFERENCES

[1] Jens Ahrens and Sascha Spors. Implementation of directional sources in wave field synthesis. In *IEEE Workshop on Applications of Signal Processing to Audio and Acoustics (WASPAA)*, New Paltz, NY, October 21-24 2007.

[2] J. Daniel. Spatial sound encoding including near field effect: Introducing distance coding filters and a viable, new ambisonic format. In *23rd International Conference, May 23–25*, Copen-

hagen, Denmark, 2003. Audio Engineering Society (AES).

[3] J. Daniel, R. Nicol, and S. Moreau. Further investigations of high order ambisonics and wavefield synthesis for holophonic sound imaging. In *114th Convention, March 22-25*, Amsterdam, The Netherlands, 2003. Audio Engineering Society (AES).

[4] Michael A. Gerzon. With-heigth sound reprodution. *Journal of the Audio Engineering Society (JAES)*, 21:2–10, 1973.

[5] J.Daniel. Représentation de champs acoustiques, application à la transmission et à la reproduction de scènes sonores complexes dans un contexte multimédia. PhD thesis Université Paris 6, 2001.

[6] H. Jones, R. Kennedy, and T. Abhayapala. On dimensionality of multipath fields: Spatial extent and richness. *IEEE Int. Conf. on Acoustics, Speech, and Signal Processing, Orlando, Florida, USA*, 2002.

[7] Poletti M., A. Three-dimensional surround sound systems based on spherical harmonics. *Journal of the Audio Engineering Society (AES)*, 53(11):1004–1025, November 2005.

[8] David Malham. Spherical harmonic coding of sound objects - the ambisonic 'o' format. In *19th International Conference, Schloss Elmau, Germany*. Audio Engineering Society (AES), May 2001.

[9] A.V. Oppenheim and R.W. Schafer. *Discrete-Time Signal Processing*. Prentice-Hall, 1989.

[10] R. Rabenstein and S. Spors. Multichannel sound field reproduction. In Benesty, J., Sondhi, M., Huang, Y, (Eds.), Springer Handbook on Speech Processing and Speech Communication, Springer Verlag, 2007.

[11] Sascha Spors. Active listening room compensation for spatial sound reproduction systems. PhD thesis, University of Erlangen-Nuremberg, 2005.

[12] Sascha Spors and Jens Ahrens. Comparison of higher-order ambisonics and wave field synthesis with respect to spatial aliasing artifacts. In *19th International Congress on Acoustics*, Madrid, Spain, 2-7 September 2007.

[13] Julius Adams Stratton. *Electromagnetic Theory*. McGraw-Hill Book Company Inc., New York, 1941.

[14] D.B. Ward and T.D. Abhayapala. Reproduction of a plane-wave sound field using an array of loudspeakers. In *IEEE Transactions on Speech and Audio Processing, Vol. 9(6)*, September 2001.

[15] E.G. Williams. *Fourier Acoustics: Sound Radiation and Nearfield Acoustic Holography*. Academic Press, London, 1999.